

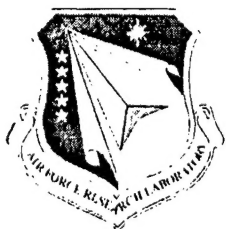
**Climatological Fit to the Ionospheric Parameters  
 $f_0F_2$  and  $h_mF_2$  for the High Latitude Stations at  
Sondrestrom, Greenland, and Qaanaaq, Greenland**

**Balkrishna S. Dandekar**

**11 July 2002**

**Approved for Public Release; Distribution Unlimited**

20040420 108



**AIR FORCE RESEARCH LABORATORY  
Space Vehicles Directorate  
29 Randolph Rd  
AIR FORCE MATERIEL COMMAND  
Hanscom AFB, MA 01731-3010**

---

This technical report has been reviewed and is approved for publication.

/ signed /

---

JOHN B. WISSLER, Lt Col, USAF  
Chief, Battlespace Environment Division

/signed /

---

BALKRISHNA S. DANDEKAR  
Author

/ signed /

---

WILLIAM E. JOY, Maj, USAF  
Chief, Ionospheric Hazards  
Specification and Forecast Section

This report has been reviewed by the AFRL/VS Public Affairs Office (PA) and is releasable to the National Technical Information Service (NTIS).

Qualified requestors may obtain additional copies from the Defense Technical Information Center (DTIC). All others should apply to the National technical Information Service.

If your address has changed, if you wish to be removed from the mailing list, or if the addressee is no longer employed by your organization, please notify AFRL/VSIM, 29 Randolph Rd., Hanscom AFB, MA 01731-3010. This will assist us in maintaining a current mailing list.

Do not return copies of this report unless contractual obligations or notices on a specific document require that it be returned.

REPORT DOCUMENTATION PAGE					Form Approved OMB No. 0704-0188	
The public reporting burden for this collection of information is estimated to average 1 hour per response, including the time for reviewing instructions, searching existing data sources, gathering and maintaining the data needed, and completing and reviewing the collection of information. Send comments regarding this burden estimate or any other aspect of this collection of information, including suggestions for reducing the burden, to Department of Defense, Washington Headquarters Services, Directorate for Information Operations and Reports (0704-0188), 1215 Jefferson Davis Highway, Suite 1204, Arlington, VA 22202-4302. Respondents should be aware that notwithstanding any other provision of law, no person shall be subject to any penalty for failing to comply with a collection of information if it does not display a currently valid OMB control number.						
PLEASE DO NOT RETURN YOUR FORM TO THE ABOVE ADDRESS.						
1. REPORT DATE (DD-MM-YYYY) 07-11-2002		2. REPORT TYPE Scientific, Interim			3. DATES COVERED (From - To) 1 Aug 2001-11 Jul 2002	
4. TITLE AND SUBTITLE Climatological Fit to the Ionospheric Parameters foF2 and HmF2 for the High Latitude Stations at Sondrestrom, Greenland, and Qaanaaq, Greenland				5a. CONTRACT NUMBER		
				5b. GRANT NUMBER		
				5c. PROGRAM ELEMENT NUMBER 621010		
6. AUTHOR(S) Balkrishna S. Dandekar				5d. PROJECT NUMBER 1010		
				5e. TASK NUMBER IC		
				5f. WORK UNIT NUMBER AA		
7. PERFORMING ORGANIZATION NAME(S) AND ADDRESS(ES) Air Force Research Laboratory/VSBXI 29 Randolph Road Hanscom AFB, MA 01731-3010					8. PERFORMING ORGANIZATION REPORT NUMBER AFRL-VS-TR-2002-1682 Environmental Research Papers, No. 1252	
9. SPONSORING/MONITORING AGENCY NAME(S) AND ADDRESS(ES)					10. SPONSOR/MONITOR'S ACRONYM(S)	
					11. SPONSOR/MONITOR'S REPORT NUMBER(S)	
12. DISTRIBUTION/AVAILABILITY STATEMENT Approved for public release; distribution unlimited.						
13. SUPPLEMENTARY NOTES						
14. ABSTRACT Ionospheric data from the high latitude stations Sondrestrom, Greenland, and Qaanaaq, Greenland, for a period of 8 years, covering a good range of solar cycle variation, are used to derive empirical algorithms for the prediction of foF2 and hmF2. The algorithm connects these two parameters with diurnal, seasonal, 90-day averaged solar flux at 2800 MHz and the planetary geomagnetic activity index Kp. The Sondrestrom station sees foF2 enhancement due to the tongue of ionization, and the Qaanaaq station experiences foF2 enhancement due to the occurrence of the polar cap patch activity. Therefore, empirical algorithms are derived for predicting the distribution of foF2 during the presence (or absence) of the polar cap patch (or tongue of ionization) activity. This algorithm connects the average and average plus or minus one sigma values of foF2 with season and 90-day averaged solar flux at 2800 MHz for the respective category. The prediction errors from these algorithms are smaller than those from the IONCAP and PRISM models. These algorithms would be very useful for filling the gaps in the real time ionospheric data needed to support USAF operational systems.						
15. SUBJECT TERMS Ionosondes    Ionosphere    Spread F    Polar cap    Algorithms						
16. SECURITY CLASSIFICATION OF:			17. LIMITATION OF ABSTRACT  UNL	18. NUMBER OF PAGES	19a. NAME OF RESPONSIBLE PERSON Balkrishna S. Dandekar	
a. REPORT UNCL	b. ABSTRACT UNCL	c. THIS PAGE UNCI			19b. TELEPHONE NUMBER (Include area code) 781 377-3298	

<b>Contents</b>	<b>Page</b>
1. Introduction	1
2. Database	2
3. Analysis	3
3.1 Climatological fit to all the data	3
3.2 Distribution of $f_0F_2$ with (or without) the presence of the polar cap patch (or TOI) activity	6
4. Interpretation	8
5. Conclusion	15
References	17

## Illustrations

## Page

Figure 1. Distribution of  $f_0F_2$  for: 1) all data, 2) with polar cap patch activity, 3) in the absence of polar cap patch activity for January 1990 at Qaanaaq.

7

Figure 2A. Empirical fit to the observed monthly parameters of peak, and width, of  $f_0F_2$  for: 1) all data, 2) the presence, and 3) absence of TOI activity at Sondrestrom.

12

Figure 2B. Empirical fit to the observed monthly parameters of peak, and width, of  $f_0F_2$  for: 1) all data, 2) the presence, and 3) absence of polar cap patch activity at Qaanaaq.

13

Figure 3. Error between autoscaled and manually scaled DISS data for the parameters  $f_0F_2$  and  $h_mF_2$  for the stations Qaanaaq and Sondrestrom.

14

<b>Tables</b>	<b>Page</b>
1. Stations Used for the Study	2
2. Data Available for the Study	3
3. Empirical Coefficients for Equation (1)	5
4. Summary of the Correlation Study	5
5. Empirical Coefficients for Equation (2)	9
6. Population of Scaled Data Using the ARTIST-4 Program for a Given Range of Error	15

**Acknowledgements:**

The author thanks Todd Pedersen for his comments, and John Heckscher for his interest in the work.

# **Climatological fit to the ionospheric parameters, $f_0F_2$ and $h_mF_2$ for the high latitude stations at Sondrestrom, Greenland and Qaanaaq, Greenland**

## **1. Introduction**

Ionospheric models such as IONCAP (Lloyd et al. 1978), International Reference Ionosphere (IRI-90, Bilitza 1990), and PRISM (Daniell et al. 1995), are used for prediction of ionospheric parameters. The models IONCAP and PRISM provide standard ionospheric parameters, whereas the models IRI-90 and PRISM are used in additional studies of the altitude dependence of the ionospheric electron density profile. Models such as PRISM provide a special capability of updating the ionospheric parameters by using a variety of real time data collected from various platforms. On the other hand, real time operational systems need relatively simple, short and robust algorithms for a prompt prediction of the ionospheric parameters as a backup for periods when the system may be temporarily degraded or inoperable. With the availability of a continuous chain of data covering a complete solar cycle, along with high computer speed for analyzing large volumes of data, it is now possible to construct relatively simple algorithms for individual stations for a prediction of ionospheric parameters for the respective locations such as those needed for the sensor based C/NOFS program launched by the US Air Force. This report presents a construction of such algorithms for  $f_0F_2$  and  $h_mF_2$  for the stations Sondrestrom, Greenland and Qaanaaq, Greenland. At the high latitude of Sondrestrom, often a tongue of ionization ((TOI) Tsunoda 1988) is seen, which is a source for the formation of polar cap patches. The polar cap station at Qaanaaq sees polar cap patch activity (see Dandekar and Bullett 1999 and references therein, Dandekar 2002). Therefore climatological algorithms for  $f_0F_2$  to provide distributions corresponding to the presence or absence of polar cap patch (or TOI) activity are also considered.

## **2. Database**

For each of the stations: Sondrestrom, Greenland and Qaanaaq, Greenland, four representative one year data sets of  $f_0F_2$  and  $h_mF_2$  for the years 1989-1990, 1991-1992, 1993-1994 and 1996-1997 are used to cover the whole range of variation over solar cycle 22 (and the beginning of solar cycle 23). Usually these data were collected at 15-minute intervals from the digital ionospheric sounding systems (DISS) (Reinisch et al. 1983) deployed at the respective



stations by the Air Force Research Laboratory, Hanscom AFB, Massachusetts, US. The  $f_0F_2$  and  $h_mF_2$  data are extracted from the ionograms by the automatic scaling program 'ARTIST-4' of the DISS system. (The accuracy of scaling by ARTIST-4 will be discussed later). The geographic and corrected geomagnetic coordinates of the stations, with relationships of local time (LT), universal time (UT), and corrected geomagnetic time (CGMLT) are listed in Table 1. Qaanaaq,  $3.3^\circ$  away from the corrected geomagnetic pole is a real polar cap station, whereas Sondrestrom at  $75.16^\circ$  corrected geomagnetic latitude (CGMLAT) is an auroral station during local day time and a polar cap station during local nighttime conditions.

Table 1. Stations used for the study

Station	Sondrestrom	Qaanaaq
Geogr. Lat.	$67.0^\circ$ N	$77.5^\circ$ N
Geogr. Long.	$50.6^\circ$ W	$68.7^\circ$ W
Corr. Geomag. Lat.	$75.16^\circ$ N	$86.71^\circ$ N
Corr. Geomag. Long.	$42.47^\circ$ E	$40.39^\circ$ E
LT at 0000 UT	2036	1924
CGMLT at 0000 UT	2154	2148
UT at 1200 LT	1524	1636

Data availability from the respective stations is presented in Table 2. The data selected are typically from July 1 to June 30 of the following year. In the top two lines the table lists the station and the parameter used for the study. The left-hand column lists the period of the data used. For each parameter the table presents the number of observations for the combined year, and as percent available of the expected data coverage. The table shows that the data availability was as low as 42% for  $h_mF_2$  at Sondrestrom in 89-90 and as high as 90% for  $f_0F_2$  at Qaanaaq in 96-97. The overall data availability is 62% for  $f_0F_2$  and 58% for  $h_mF_2$  at Sondrestrom, and 78% for  $f_0F_2$  and 76% for  $h_mF_2$  at Qaanaaq. The averaged sunspot numbers (SSN) with the standard error, for the respective periods in Table 2 are  $149 \pm 49$ ,  $127 \pm 51$ ,  $38 \pm 22$ , and  $10 \pm 10$  respectively. Thus the data used form a good sample covering the whole range of the solar cycle change. Auxiliary data such as  $K_p$ , sunspot number (SSN) and solar flux ( $w/cm^2 s^{-1}$ , at 2800 MHz) used in the analysis were available from the World Data Center, Boulder, Colorado.

Table 2. Data available for the study

Station	Sondrestrom				Qaanaaq			
Parameter	$f_0F_2$		$h_mF_2$		$f_0F_2$		$h_mF_2$	
Year	No. of obs.	%	No. of obs.	%	No. of obs.	%	No. of obs.	%
89-90	15920	45	14756	42	29698	85	29182	83
91-92	21974	63	20609	59	22545	64	21509	61
93-94	26862	77	25075	72	26308	74	25694	73
96-97	22644	65	20635	59	31548	90	30880	88
Total	87400	62	81075	58	109829	78	107265	76

### 3. Analysis

#### 3.1 Climatological fit to all the data

As a starting point, the determination of an empirical fit to  $f_0F_2$  and  $h_mF_2$  data from Sondrestrom and Qaanaaq, without any consideration of the TOI or polar cap patch activity, is conducted by using an equation of the form,

$$\begin{aligned}
 f_0F_2 \text{ (or } h_mF_2) = & A_0 \\
 & + A_1 F \\
 & + A_2 \sin((H - H_0) * 15^\circ * \pi / 180^\circ) \\
 & + A_3 \cos(0.5 (D - D_1) (360/366) * \pi / 180^\circ) \\
 & + A_4 \cos((D - D_2) (360/366) * \pi / 180^\circ) \\
 & + A_5 K_p
 \end{aligned} \tag{1}$$

where,

$A_0$  to  $A_5$  are empirical coefficients,

$H_0$ ,  $D_1$ , and  $D_2$  are empirical constants

$H$  is the universal time (U. T.) in hours,

$D$  is the incremental calendar day, taking into account the time for the observation,

$F$  is the solar flux in  $\text{w/cm}^2 \text{ s}^{-1}$  measured at 2800 MHz, and averaged for 90 days prior to the day of the ionospheric observation,

$K_p$  is the index of planetary magnetic activity, and

the term  $\pi / 180^\circ$  converts the respective angles in degrees to radians.

The multiplication terms of coefficients  $A_1$  to  $A_5$  represent the dependence of  $f_0F_2$  (or  $h_mF_2$ ) on solar flux, diurnal, semiannual and annual variation, and dependence on the index  $K_p$  of planetary magnetic activity respectively.

All the needed empirical constants and coefficients in Eq.(1) were determined by using data from all four years, summarized in Table 2 with the SVDC routine of the Interactive Data Language (IDL 1995, reference guide) computer programs. For each station and each parameter, a contribution from every term in Eq.(1) is estimated.

The terms contributing less than 10 percent are dropped, and the remaining constants and coefficients are recomputed. The final terms used for the fit are presented in Table 3. After all the constants in Eq.(1) are determined, one can calculate the contribution of each term of Eq.(1), and its percent contribution to the ionospheric parameter under study. These relative contributions are also presented in Table 3. The top two lines in Table 3 list the parameter and the station. The next three lines present the constants determined for Eq.(1) for the respective parameter and station. The next six lines present the computed values of the coefficients A0 to A5. For the coefficients, each column is subdivided into two columns. The first column lists the magnitude of the coefficient and the second column gives the percent contribution of the respective term to that ionospheric parameter. It is observed that in Eq.(1), solar flux averaged for 90 days (3 months) prior to the day of ionospheric observation provides a better fit than that based on the use of daily solar flux. Therefore the coefficients derived with use of 3 months' averaged solar flux are listed in the Table 3.

At the bottom of Table 3, each top column is subdivided into three columns. The left-hand column describes the item for the fit of Eq.(1). For each parameter there are three entries; 1) standard error in MHz (or km), 2) shift in the fit with respect to the observed values, and 3) standard error as percent. Similarly the errors between observations and predictions from the IONCAP and PRISM models were computed and summarized in the bottom lines in Table 3. The table shows that the fit by use of Eq.(1) (third line from the bottom in Table 3) has smaller error than from either the IONCAP (second line from the bottom in Table 3) or the PRISM (last line in Table 3) models.

Correlation coefficients were computed between  $f_0F_2$  (or  $h_mF_2$ ) and the respective parameter on the right side in Eq.(1) and are presented in Table 4. The parameters are listed in the left-hand column. Two columns on the right-hand side are for two stations. Each station column is divided into two columns for the parameter  $f_0F_2$  and  $h_mF_2$ . The partial correlation coefficients are shown in the table. Two lines at the bottom of the table list the total correlation coefficient and the percent volume of the correlated data ( $C^2$  to C, where C is the coefficient of

correlation). The total correlation coefficients are very significant ( $\geq 0.707$ ), showing that the correlated population ranges from 43 to 75 percent.

Table 3. Empirical Coefficients for Equation 1.

Parameter	f <sub>0</sub> F <sub>2</sub>					h <sub>m</sub> F <sub>2</sub>						
Station	Sondrestrom			Qaanaaq		Sondrestrom			Qaanaaq			
Constant												
H0	10.5			13.25		8.0			10.5			
D1	177			176		178			173			
D2	--			--		181			173			
Coefficient												
A0	2.152	%	1.458	%	182.39	%	199.34	%				
A1	0.0163	36	0.01658	40	0.4798	24	0.352	17				
A2	1.1056	32	0.532	17	-29.95	20	-20.27	13				
A3	0.895	14	1.594	27	68.2	24	80.6	28				
A4					-50.12	33	-69.04	43				
A5	-0.0143	18	-0.01272	17								
Standard error σ from												
	MHz	MHz	%	MHz	MHz	%	Km	Km	%	Km	Km	%
Obs.	1.56	Shift		1.48	Shift		59.6	Shift		52.4	Shift	
Eq.(1) Fit	1.03	0.003	23	0.99	-0.001	24	41.8	0.04	18	37.6	0.09	13
IONCAP	1.1	0.16	26	1.12	0.27	30	52.7	35.2	22	51.3	38.2	20
PRISM	1.09	0.32	25	1.03	0.18	28	58.5	18.1	23	46.2	19.5	18

Table 4. Summary of Correlation Study

Station	Sondrestrom		Qaanaaq	
Parameter	$F_0F_2$	$h_mF_2$	$f_0F_2$	$H_mF_2$
Dependence on	Partial coefficient of correlation			
Flux	0.5143	0.4943	0.6080	0.4352
Diurnal	0.4799	-0.3596	0.2336	-0.2685
Semiannual	0.0791	-0.2763	0.2656	-0.4588
Annual		-0.2999		-0.4925
Kp	0.0303		-0.0153	
Total Corr. Coeff.	0.7504	0.6599	0.7441	0.6972
Correlated population (%)	56 – 75	43 – 66	55 – 74	49 – 70

Residual errors were examined to see if these show any systematic behavior, which might indicate a systematic time dependent under- or over-estimate. Because no such behavior was found, no further correction to the algorithm could be made.

### 3.2 Distribution of $f_0F_2$ with (or without) the presence of polar cap patch (or TOI) activity

As the high latitude stations see the polar cap patch activity at Qaanaaq and the formation of a tongue of ionization (TOI) at Sondrestrom, one would like to quantify  $f_0F_2$  distributions in these two groups. For the polar cap patch study, Dandekar (2002) suggested a procedure of subtracting an averaged background for determining the polar cap patch (or TOI) activity. Dandekar (2002) treated short duration peaks (less than 30 minutes, that is, at least two consecutive observations) as jitter in the data. As the high latitude station Qaanaaq sees a lot of short duration polar cap patches (seen from 1-minute interval observations); the process of counting these peaks and their durations is modified for this analysis.

The goal here is to separate the data into two groups a) with the presence and b) absence of the polar cap patch (or TOI) activity. The monthly distributions of all  $f_0F_2$  data are divided into bins, each with a width of 0.1 MHz. It is observed that these distributions do not strictly follow the Gaussian distribution (the Gaussian distribution is defined by two terms: the root mean squared value (RMS) and the standard error for the given set). Therefore, the mode and median distributions are also used for the analysis. Because the selected interval of 0.1 MHz is reasonably narrow, and the distribution is not necessarily smooth, the modal (highest occurrence) value was determined by averaging  $f_0F_2$  for the three highest occurrences. The values  $\geq 1.1 \cdot \text{RMS} (\text{/mode/median}) f_0F_2$  are assumed to be due to the polar cap patch (or TOI) activity. The base of the polar cap patch is assumed to be equal to  $0.8 \cdot \text{RMS} (\text{/mode/median}) f_0F_2$ . Also, the duration of a polar cap patch was assumed to be  $\leq 2$  hours. With these criteria, the monthly data are scanned to determine the distribution of  $f_0F_2$  for the occurrence of polar cap patch activity. The monthly distribution of  $f_0F_2$  in the absence of polar cap patch (or TOI) activity was computed by subtracting this  $f_0F_2$  distribution from the monthly distribution of all the data. For the Gaussian distribution, the error of  $\pm 1\sigma$  covers 68% of the data population. In using the mode and median methods, the corresponding range points were determined. As the results from median and mode methods did not show any systematic and significant differences from those from the Gaussian distribution, the latter method (Gaussian distribution) is used in this analysis. As an example the  $f_0F_2$  distributions for January 1990 for Qaanaaq are shown in Figure 1. Three curves show the distributions of  $f_0F_2$  for 1) all data (dotted), 2) presence of polar cap patches (dashes) and 3) absence of the polar cap patches (dash dot dash). The corresponding vertical lines mark the peaks

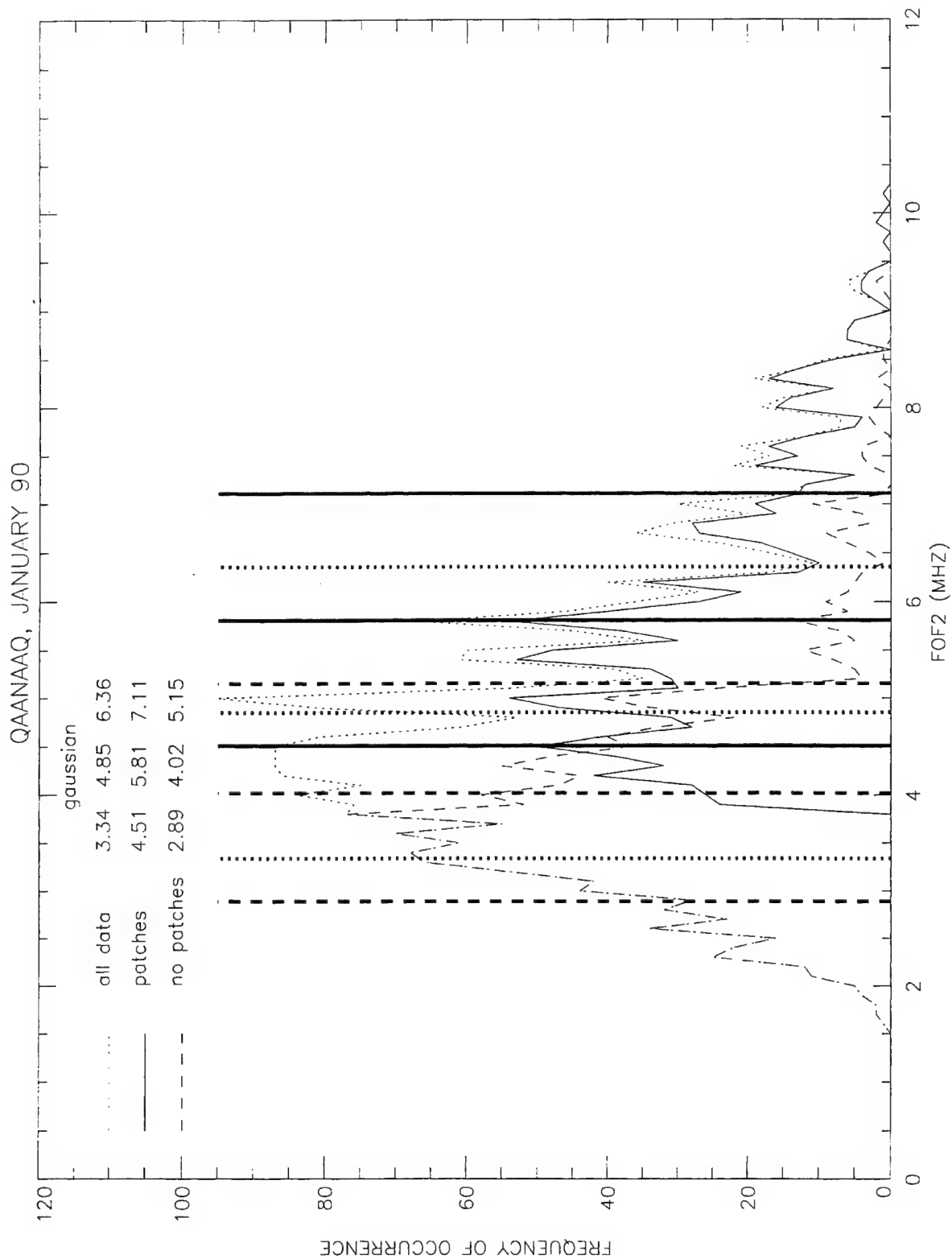


Figure 1. Distribution of  $f_0F_2$  for: 1) all data, 2) with polar cap patch activity, 3) in the absence of polar cap patch activity for January 1990 at Qaanaaq. Below 3.8 MHz, the curve for no patches and the curve for all data merge.

and widths for the respective category. The curve corresponding to the presence of polar cap patches is the right hand part of the curve and the curve corresponding to the absence of the polar cap patches is the left hand part of the curve. Because of the narrow width of 0.1 MHz for the bins, all these curves show some jitter. The  $f_0F_2$  values are also listed in the figure for convenience. Three columns present average  $-\sigma$ , average, and average  $+\sigma$ , respectively, for the condition listed on the left hand side of the columns. One would expect higher  $f_0F_2$  for polar cap patch activity and lower  $f_0F_2$  in the absence of polar patch activity with respect to distribution of all the data as seen in the figure.

The values of  $f_0F_2$  for peak (RMS) occurrence are determined for 1) all the data, 2) background (absence of activity), and 3) the presence of activity. The widths ( $\sigma$ ) for the corresponding groups are determined. Thus there are two parameters; ( $f_0F_2$  peak, and width in MHz) for each group. An algorithm

$$\text{Peak (or width } f_0F_2) = B_0 + B_1 \cos((\text{mon}-\text{mon}_0) * \text{FAC} * \pi / 180^\circ) + B_2 F \quad (2)$$

is used,

where  $B_0$ ,  $B_1$ ,  $B_2$ , are empirically determined coefficients, and

$\text{mon}_0$  and  $\text{FAC}$  are empirically determined constants,

$\text{mon}$  is the month of the observation,

$F$  is the solar flux (averaged over 90 prior days) in  $\text{w/cm}^2 \text{ s}^{-1}$  measured at 2800 MHz, and

the term  $\pi / 180^\circ$  converts the respective angles in degrees to radians.

THE SVDC routine mentioned above is used to determine the empirical constants in Eq.(2). For simplicity  $\text{mon}_0 = 6$ , and  $\text{FAC}=15$  is used for the whole data set. The results are summarized in Table 5.

#### 4. Interpretation:

The distance between the stations Sondrestrom and Qaanaaq is 1306 km. The asymmetrical characteristics of the auroral oval with respect to the magnetic north pole makes Sondrestrom, at  $75.16^\circ$  corrected geomagnetic latitude (CGMLAT), an auroral station during local daytime and a polar cap station during the local nighttime conditions, whereas Qaanaaq, at

Table 5. Empirical Coefficients for Equation 2

Station		Sondrestrom				Qaanaaq			
Coefficient		B0	B1	B2	Standard Error (MHz)	B0	B1	B2	Standard Error (MHz)
Item									
Peak $f_0F_2$ (MHz)	All Data	2.088	0.855	0.015	0.308	1.301	1.590	0.016	0.423
	Patches	2.789	0.344	0.019	0.426	1.731	1.243	0.019	0.486
	Back-Ground	1.766	1.14	0.013	0.265	1.044	2.034	0.013	0.388
Width (MHz)	All Data	0.628	-0.364	0.006	0.225	0.566	-0.459	0.005	0.198
	Patches	0.616	-0.515	0.005	0.227	0.526	-0.366	0.004	0.164
	Back-Ground	0.374	-0.053	0.005	0.228	0.398	-0.22	0.004	0.214

3.3° away from the corrected geomagnetic pole, is a true polar station at all times. These two stations see different ionospheric features. Sondrestrom sees the tongue of ionization (TOI). Under favorable interplanetary magnetic field (IMF) conditions, the TOI breaks into polar cap patches and these patches drift northward (poleward) to Qaanaaq (see Dandekar and Bullett 1999, Basu and Valladares 1999, and references therein). Against this background let us look at the results summarized in Table 3.

The peak in diurnal variation of  $f_0F_2$  (or  $h_mF_2$ ) is a quarter of the day; that is six hours after H0, and is to be added to the constant H0. Thus according to Eq.(1)  $f_0F_2$  peaks at Sondrestrom around 1630 (10.5+6) UT, and the peak at Qaanaaq occurs around 1915 (13.25+6) UT. The delay in the occurrence of the peak of  $f_0F_2$  between the two stations is consistent with the observation that the polar cap patches are formed from the tongue of ionization (TOI) at the latitude of Sondrestrom, and drift towards the pole to Qaanaaq.

The constants D1 and D2 for the semiannual and annual variation are practically the same. Note that the annual component is weak (absent, A4~0) for  $f_0F_2$  at both the stations. The constant A1 is same for both the stations. The presence of the constant A5 shows a magnetic control ( $K_p$ ) on  $f_0F_2$  at both stations.

The respective coefficients for  $h_mF_2$  for both the stations are in reasonable agreement with each other. Note that altitude dependence shows an annual component (A4), but weak magnetic dependence (A5~0).



The bottom section of the table compares the fit of Eq.(1) with that from the IONCAP and PRISM models. The IONCAP and PRISM models are based on data mostly collected during solar cycle 19 (International Geophysical year IGY 1957). The table shows that the standard error (both in magnitude and as percent error) as well as the shift is smallest from the algorithm. The IONCAP model on the average underestimates the altitude by 35 km. The PRISM model underestimates it by 15 km, in spite of the fact that it incorporates quite a few more parameters than those used in the IONCAP program for ionospheric predictions. The strength of the PRISM model lies in the fact that the results can be updated by using real time data from various platforms.

A correlation study was conducted between the items (multiplying terms for the coefficients) listed in Table 3 and the observations of  $f_0F_2$  and  $h_mF_2$ . The results are summarized in Table 4. The table presents partial correlation coefficients for the items shown in the left-hand column for the stations listed on the top line, and for the parameter listed on the second line from the top. The bottom line shows the total correlation coefficient for the parameter listed on line 2 from the top, with the relevant items in the left-hand column used. Note that items contributing less than 10% (see Table 3) are not used. The larger the magnitude of a partial correlation coefficient in a given column, the larger the contribution the item makes to the parameter. The second row from the bottom lists the correlation between observations and the fit from Eq.(1). This row shows that when the most relevant items are combined, they produce a significant level of correlation ( $\geq 0.707$ ), indicating an overall improvement in the dependence of the parameter on the chosen terms. The last row presents the range ( $C^2$  to  $C$ , where  $C$  is the coefficient of correlation) of percent population showing covariation. At Sondrestrom this range is a little lower for  $h_mF_2$ . All others have a good range (at least 50%) of the population showing a good co-variation.

Equation 2 is used to determine the coefficients presenting the distribution of general population and background (absence of polar cap patches) and polar cap patch activity at Qaanaaq and TOI activity at Sondrestrom. These are summarized in Table 5. The table is divided into three major columns, the first for listing the items and the other two for the stations Sondrestrom and Qaanaaq. The first column is subdivided in two columns; the first lists the parameter under study and the second column describes the category. For each station the major column is subdivided into four columns to present the empirical coefficients B0, B1, B2, and the

standard error for the empirical fit to the data. For simplicity the reference month, mon0, and the factor FAC in Eq.(2) are fixed at 6 and 15 respectively for all the data in the set. The term multiplying the coefficient B2 is F, the solar flux. As the 90-day average solar flux before the day of ionospheric observation is found to produce better results than that from using daily solar flux, the former is used in the computations.

The results are shown in Figures 2A and 2B for Sondrestrom and Qaanaaq respectively. Each figure has six panels. Each row presents results for all data, for polar cap patch activity and absence of polar cap patch activity. Along the column are the parameters: peak, and width for the category of the row. In each panel the horizontal axis presents months of observation as a continuous sequence, and the numbers just above the axis show the calendar year for the observations. In each panel the continuous curve shows the observed dependence and the dotted curve shows the empirical fit. In each panel the numbers on the left-hand side, from the top to the bottom, list the coefficients and standard error respectively in the empirical fit of Eq.(2). In each panel, the comparison of the pairs of curves shows that the empirical fit is very reasonable, in spite of a factor of 2 variation in both the peak and the width of the distribution of  $f_0F_2$  for the respective category, over a period of 9 years. Thus these algorithms would be very useful to operational systems for estimating  $f_0F_2$  when real time observational data are not available.

In the above analysis, the automatically scaled data from the DISS systems are used under the assumption that this scaling is reasonably accurate. For validating this hypothesis, the auto-scaled data were compared with manually scaled data. The results are presented in Figure 3. The four panels in Figure 3 present observed errors as histograms for  $f_0F_2$  and  $h_mF_2$  for the stations Qaanaaq and Sondrestrom. The data for one week of November and one week of December 1993 were used. The selected year is listed at the top of each block. The left-hand top corner in each block lists the number of ionograms available for comparison. The results are summarized in Table 6. The table shows that accuracy in auto scaling of frequency is acceptable, whereas the accuracy in auto scaling of altitude is marginal. These errors would superpose on the errors in the algorithm shown in Tables 3 and 5.

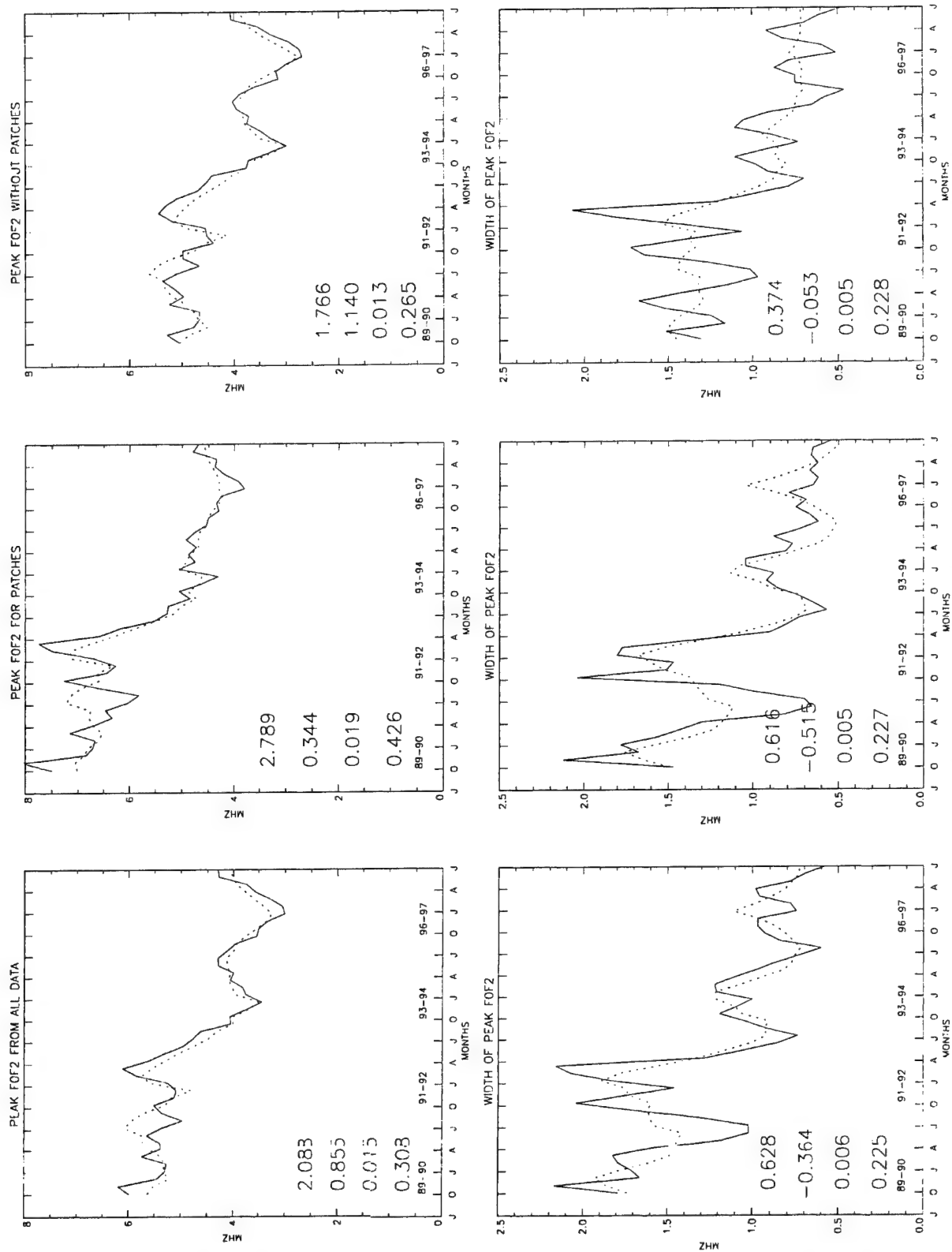


Figure 2A. Empirical fit to the observed monthly parameters of peak, and width, of  $f_0F_2$  for: 1) all data, 2) the presence, and 3) absence of TOI activity at Sondrestrom.

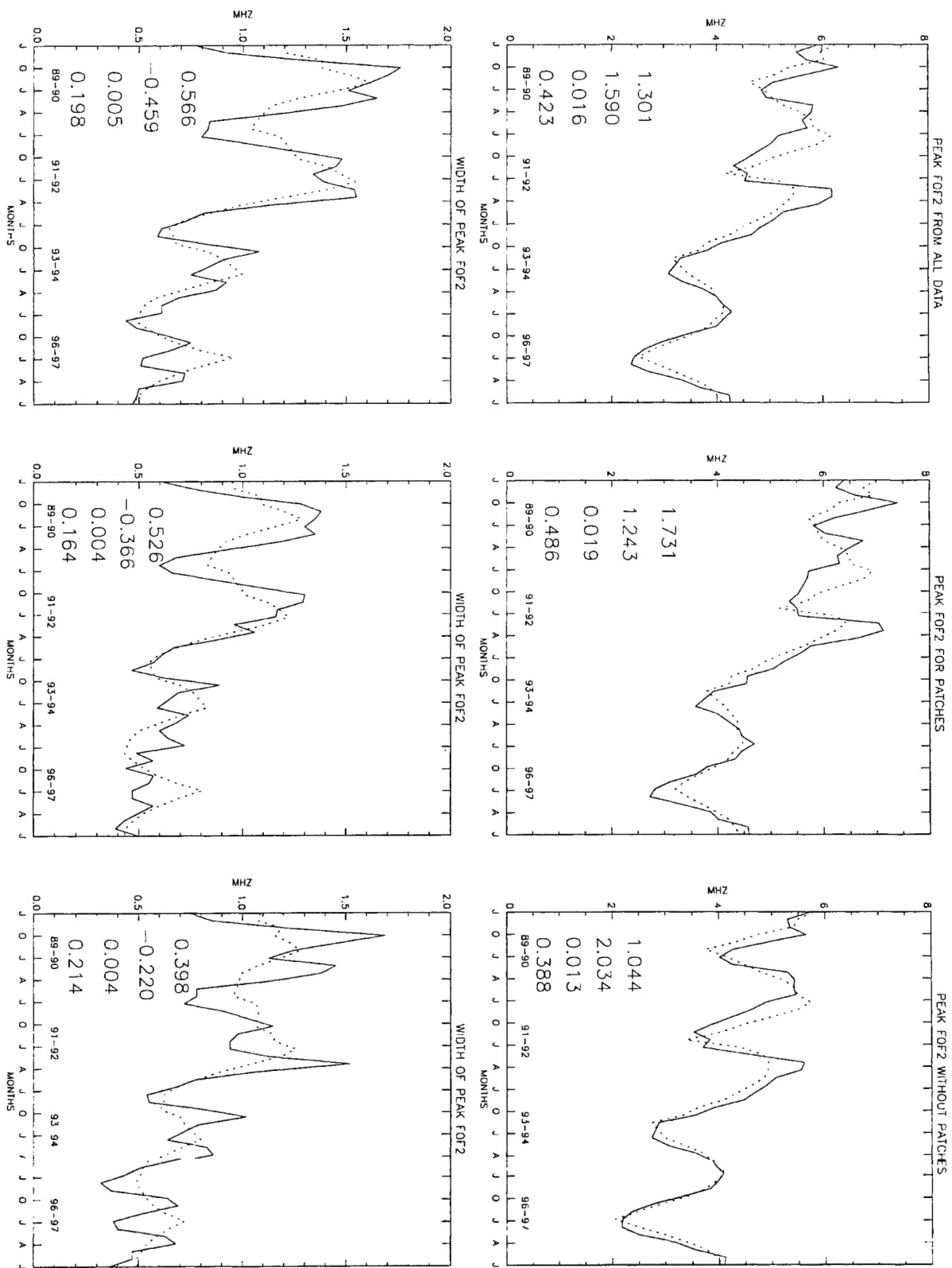


Figure 2B. Empirical fit to the observed monthly parameters of peak, and width, of  $f_0F_2$  for: 1 (all data, 2) the presence, and 3) absence of polar cap patch activity at Qaanaaq.

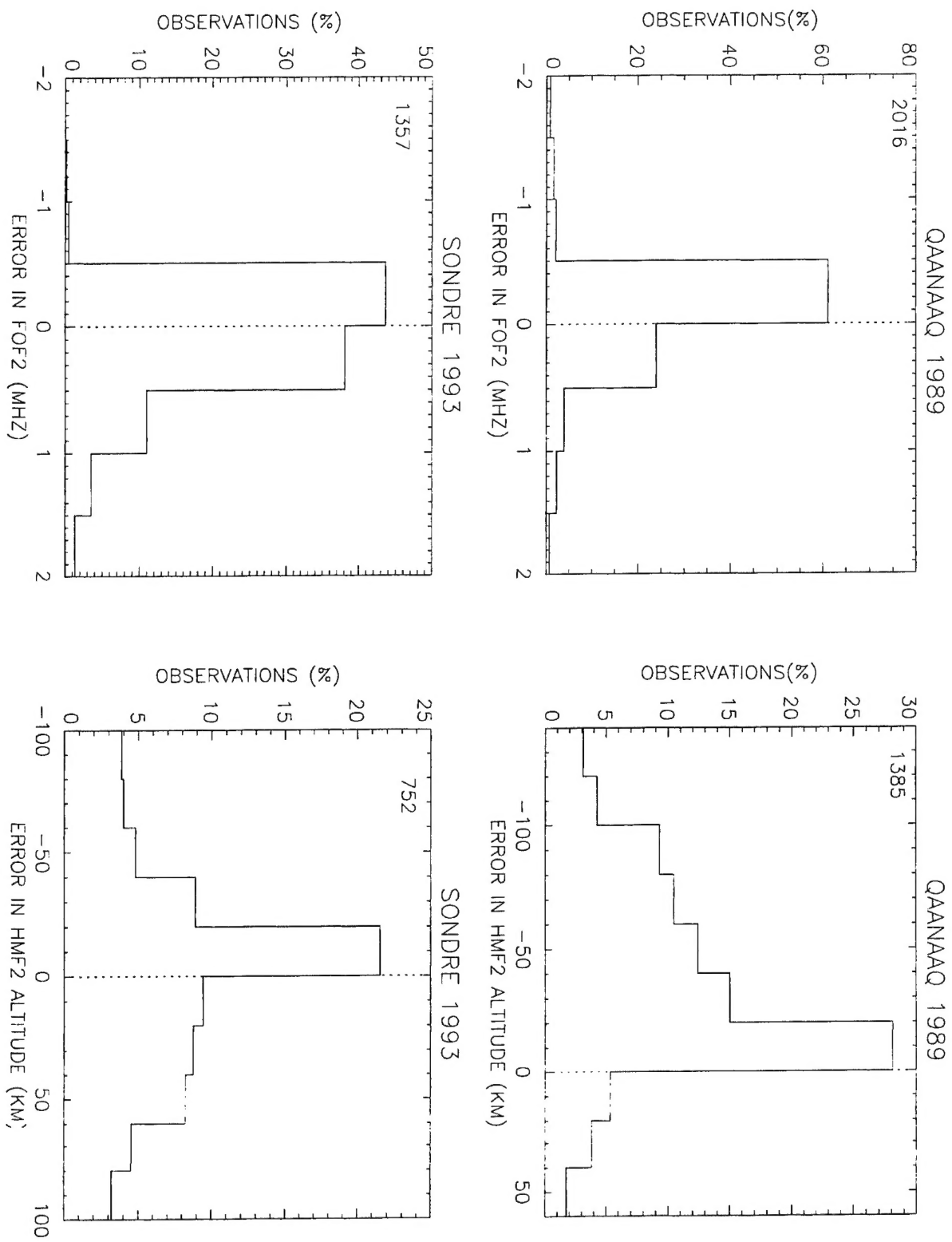


Figure3. Error between autoscaled and manually scaled DISS data for the parameters  $f_0F_2$  and  $h_mF_2$  for the stations QAANAQ and Sondrestrom.

Table 6. Population of data scaled using the ARTIST-4 program for a given range of error

Parameter	Error (MHz)	f <sub>0</sub> F <sub>2</sub>		Error (km)	h <sub>m</sub> F <sub>2</sub>	
Station		Sondrestrom	Qaanaaq		Sondrestrom	Qaanaaq
Year		1993	1989		1993	1989
		Percent data covered			Percent data covered	
		0.5	81		85	20
	1.0	93	91	40	48	52
	1.5	96	95	60	61	66
				80	70	77
				100	77	81

## 5. Conclusion

Customized algorithms derived by empirical fit to historical data for individual stations work better than the models used for global predictions. The next possible step in improving the present algorithm in Eq.(1) is to subdivide the diurnal, semiannual, and annual variations presented by a single (sine, cosine) function, into several sections by using a spline technique (Boor 1978). Another possibility is to put additional parameters into the empirical equations to improve the accuracy of prediction. These relatively simple algorithms should be incorporated in models like PRISM for improving global predictions.

The high latitude stations selected here also see special features such as the tongue of ionization at Sondrestrom and polar cap patch activity at Qaanaaq. An additional algorithm in Eq.(2) quantifies the  $f_0F_2$  distributions for the respective periods, and would be useful to operational systems, which are often degraded during disturbances associated with these phenomena.

## References

- Basu Su., and C Valladares, 1999, Global aspects of plasma structures, *JATP*, **61**, pp127-139.
- Bilitza D., *International Reference Ionosphere* 1990, NSSDC/WDC-A-RS Rep.90-22, Goddard Space Flight Center, MD., 1990
- Boor C., 1978, *A practical guide to splines*, Springer-Verlag, New York.
- Dandekar B. S., and T. W. Bullett, 1999, Morphology of polar cap activity, *Radio Sci.*, **34**(5), pp. 1187-1205
- Dandekar B. S., 2002, Solar cycle dependence of polar cap patch activity, *Radio Sci.* **37**(1), 10.1029/2000RS002562.
- Daniell R. E., Brown L. D., Anderson D. A., Fox M. W., Doherty P.H., Decker D. T., Sojka J. J., and Schunk R. W., 1995, Parameterized ionospheric model: A global parameterization based on first principles models, *Radio Sci.*, **30**(5), pp.1499-1510.
- IDL user's guide, Interactive Data language*, 1995, Version 4, Research Systems Inc., Boulder, Colorado.
- Lloyd J. L., G. W. Haydon, D.L. Lucas and L. R. Teters, 1978, *Estimating the performance of telecommunication systems using the ionospheric channel*, National Telecommunications and Information Administration, Institute for Telecommunication Sciences, Boulder, Colorado 80303.
- Reinisch B. W., R. R. Gamache, J. S. Tang, and D. F. Kitrosser, 1983, *Automatic Real Time Scaler with True Height Analysis*, AFGL-TR-83-0209, Air Force Geophys. Lab., Bedford, Mass., , ADA122174
- Tsunoda R. T., 1988, High latitude F region irregularities: A review and synthesis, *Rev. Geophys.*, **26**(4), 729-760.